

Thermal Performance Analysis of Plaster Reinforced with Raffia Vinifera Particles for Use as Insulating Materials in Building

Etienne Malbila^{1,2*}, Danielle Manuella Djouego Tagne³, Bouto Kossi Imbga^{2,4},
Lareba Adelaide Ouedraogo², Sié Kam², David Yemboini Kader Toguyeni^{5,6}

¹Ecole Supérieure d'Ingénierie (ESI), Université de Fada N'Gourma, Fada N'Gourma, Burkina Faso

²Laboratoire d'Energies Thermiques Renouvelables (LETRE), Université Joseph KI-ZERBO, Ouagadougou, Burkina Faso

³Institut Supérieur des Techniques Industrielles et Commerciales (ISTIC), Bangangté, Cameroun

⁴Unité de Formation et de Recherche en Sciences et Technologies (UFR/ST), Université Norbert ZONGO, Koudougou, Burkina Faso

⁵Laboratoire de Physique et Chimie de l'Environnement (LPCE), Université Joseph KI-ZERBO, Ouagadougou, Burkina Faso

⁶Ecole Polytechnique de Ouagadougou (EPO), Ouagadougou, Burkina Faso

Email: *t.emalbila@gmail.com

How to cite this paper: Malbila, E., Tagne, D.M.D., Imbga, B.K., Ouedraogo, L.A., Kam, S. and Toguyeni, D.Y.K. (2024) Thermal Performance Analysis of Plaster Reinforced with Raffia Vinifera Particles for Use as Insulating Materials in Building. *Journal of Minerals and Materials Characterization and Engineering*, **12**, 112-138.

<https://doi.org/10.4236/jmmce.2024.122009>

Received: February 2, 2024

Accepted: March 26, 2024

Published: March 29, 2024

Copyright © 2024 by author(s) and Scientific Research Publishing Inc.

This work is licensed under the Creative Commons Attribution International License (CC BY 4.0).

<http://creativecommons.org/licenses/by/4.0/>



Open Access

Abstract

The present study focuses on the formulation of new composite consisting of plaster and raffia vinifera particle (RVP) with the purpose to reducing energy consumption. The aim of this study is to test this new compound as an insulating eco-material in building in a tropical climate. The composites samples were developed by mixing plaster with raffia vinifera particles (RVP) using three different sizes (1.6 mm, 2.5 mm and 4 mm). The effects of four different RVP incorporations rates (*i.e.*, 0wt%, 5wt%; 10wt%; 15wt%) on physical, thermal, mechanicals properties of the composites were investigated. In addition, the use of the raffia vinifera particles and plaster based composite material as building envelopes thermal insulation material is studied by the habitable cell thermal behavior instrumentation. The results indicate that the incorporation of raffia vinifera particle leads to improve the new composite physical, mechanical and thermal properties. And the parametric analysis reveals that the sampling rate and the size of raffia vinifera particles are the most decisive factor to impact these properties, and to decreases in the thermal conductivity which leads to an improvement to the thermal resistance and energy savings. The best improvement of plaster composite was obtained at the raffia vinifera particles size between 2.5 and 4.0 mm loading of 5wt% (C95P5R) with a good ratio of thermo-physical-mechanical properties. Additionally, the habitable cell experimental thermal behavior, with the new raffia vinifera particles and plaster-based composite as thermal insulating material for building walls,

gives an average damping of 4°C and 5.8°C in the insulated house interior environment respectively for cold and hot cases compared to the outside environment and the uninsulated house interior environment. The current study highlights that this mixture gives the new composite thermal insulation properties applicable in the eco-construction of habitats in tropical environments.

Keywords

Fibres, Plaster, Thermal Test, Mechanical Test, Insulating Material, Indoor Comfort

1. Introduction

The promotion of sustainable development must be taken into account by each sector of activity while maintaining responsible energy consumption at a minimum threshold in order to protect the environment. Energy consumption in building project comes from all steps of the construction life cycle. The construction sector accounts for a significant portion of world's global energy consumption and a third of the world's total carbon dioxide (CO₂) emissions, thus impacting the environment. Almost half of the energy loss occurs through the building envelope due to heat transfer to and from the surroundings [1] and nearly 50% of the resources extracted from the ground [2] [3]. The development of green building allows at the same time to minimize energy consumption, to reduce the natural resources exploitation and the harmful effects on the environment. For this, one way is to use new thermal insulation and sound-absorbing materials for buildings replacing the synthetic or petrochemical insulation materials [4] [5] and the reuse of end-of-life materials [6]. In addition, it enhances the use of local materials and secondary resources providing good thermal insulation [7] while ensuring the building indoor comfort. The use of agro, renewable and environmentally friendly materials as insulation materials for building walls will share in energy saving [8] and low environment impact [4] [9]. Indeed, the design of an energy-efficient envelope aims to reduce the building energy consumption, as studied by [10] and to ensure the thermal comfort of the occupants by taking into account several design variables such as geometry, material properties and the envelope dimensions, the air conditioning system and the internal load. However, these variables are inextricably linked from the perspective of the building envelope thermal optimization [1]. Therefore, it is necessary to design an optimal building envelope to reduce energy consumption in buildings that depend on several parameters, by studying the properties of building materials in which solar absorptivity, moisture permeability and insulation type are the most influential thermal variables [1]. Several researches provide an approach to evaluate the most appropriate building system to be selected in the early stages of design, leading to the use of a more environmentally, economically and socially sustainable building material [11] and new application model to regulate energy consumption in

building [12]. Faced with these constraints, we have seen in recent years, research efforts in the development of new construction methods using local materials in order to provide an adequate response to this crisis in developing countries. As such, we can note the tendency to use natural fibres as an ecological filler in the manufacture of polymer composites is increasing and constitutes an interesting research subject because of their availability, their good environmental properties [13] [14] and their competitiveness when used in large quantities [3]. There are many types of natural fibres or cellulose fibres such as date palm and hibiscus fibres, rice husks, Agave fibres, wheat straw fibres, fonio straw, Bamboo organosolv pulp, recycled waste carton pulp, etc. Although, they have lately gained popularity as an alternative component for composite material among researcher, engineers and scientist [15]. The use of natural fibres is not hazardous to human beings [16] [17]. For example, the Eucalyptus Globulus leaves as a new thermal insulating and sound absorbing material for buildings [18]. These materials have low environmental impact by using renewable natural resources for thermal insulation in buildings rather than the synthetic insulation materials.

With this in perspective, we directed our research into the thermal insulation in building with a composite material of plaster and raffia vinifera. Natural fiber composites are considered low cost composite products that can impart structural properties, and can be considered as alternative fillers to replace synthetic fibres in the manufacture of composites [13] [19] and which meet the requirements of the circular economy [3] [20].

Plaster is an available and coveted material for various uses thanks to its many advantages in the field of the building's thermal insulation with a thermal conductivity between 0.30 to 0.40 (W/m·K) [4]. However, it is fragile and sensitive to humidity, and it does not resist to flexural stresses. Therefore, for an efficient use of this material, it is necessary to reinforce it, hence the use of bamboo particles of palm of raffia vinifera. As far as raffia vinifera is concerned, its anatomy allows it to be classified in the category of soft and light woods. It is used in the fields of crafts industry [5]. The valorization of raffia vinifera fibres in insulating construction materials could be interesting for economic (diversification of the value chain) and durability reasons because of their availability, renewability and low cost in some tropical countries. Improving the properties of natural materials, manufactured and industrial and agricultural by-products constitutes an alternative to have adequate and ecological construction materials. We can mention the addition of salt [21] sand [22], date palm fibres, [13] of glass powder [23], biopolymer [3] and composites [24]. Indeed, in 2005 the content of a natural insulation represents around 5% in insulating materials used in the construction area [7] and this indicates how insulating material are important in our daily life [16]. The current tests indicate the feasibility of using such hybrid samples as insulating materials for heat as well as sound absorption [25].

In addition, the various studies carried out on these two materials reveal a positive impact on the environment, thereby respecting the principles of sustainable development. The aim of this work is to study the technical feasibility of

plaster composite materials with the incorporation of raffia vinifera particles for use as insulating materials in building. The intention is to obtain the high thermal performance and the suitable flexural strength and physical properties. Thus, the present study proposes to formulate a raffia vinifera particles and plaster composite eco-material stem according to the sampling area and the size of the fibres; and to characterize its capacity of thermal insulation of the habitable cell envelopes in the atmospheres of a tropical climate.

2. Material and Methods

The new sustainability framework for building applications takes into account social parameters, life cycle analysis and occupant satisfaction [1]. The present study is part of this dynamic and addresses the formulation and characterization of materials which constitute a basis for the analysis of the life cycle. The following paragraphs therefore present the raw materials, the formulation and the characterization protocol for the Raffia vinifera particles and plaster composite material and the instrumentation of its thermal behavior.

2.1. Raw Materials

Two basic materials are used, namely plaster as a matrix and raffia vinifera fibres as a natural stabilizer for reinforcement. The plaster used is of the usual semi-hydrated type and the fibres from the site of Mlem at 5°25'32.9" of North latitude and 10°26'09.1" East longitude. In fact, the Plaster is a construction material widely used for its good properties [26].

The raffia stem is divided into four (04) zones as shown in **Figure 1** and its properties vary according to these zones [27]. Hence the interest of taking it into account in the characterization as can be seen with the values given in **Table 1**, where the density of the raffia decreases from the periphery towards the center.

Figure 2 shows, from a radial section of the raffia, the preparation of the sampling of the natural stabilizer without particular treatment. In practice, the fibres are manufactured by using a machete for cutting and a saw for the separation into different zones, in particular the removal in the longitudinal direction of the $\frac{3}{4}$ part on the bamboo. **Figure 3** shows the raffia samples obtained after sieving

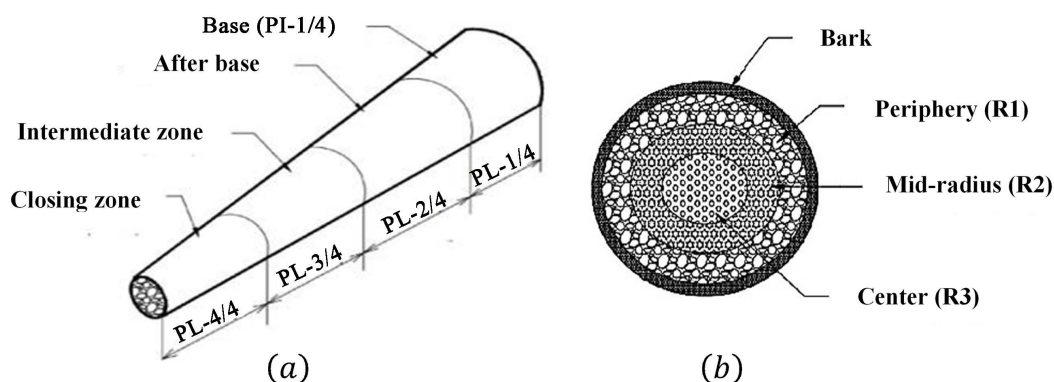


Figure 1. Sampling area (a) longitudinal section, (b) radial section [27].

and grouped according to the granulometry by zone.

2.2. Formulation and Manufacture of the Composite Material

Various formulation methods are practiced in building materials technology. This study uses the method of shaping by cold contact molding which respects the general principle of molding processes for composite materials represented in the flowchart in **Figure 4**.

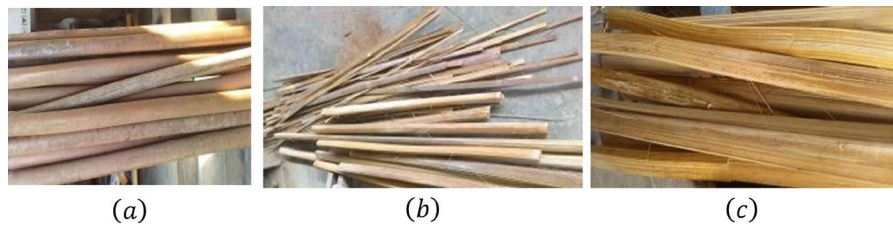


Figure 2. Sampling preparation, (a) dry bamboo; (b) separation of hulls from piths, (c) overview of bamboo pith.

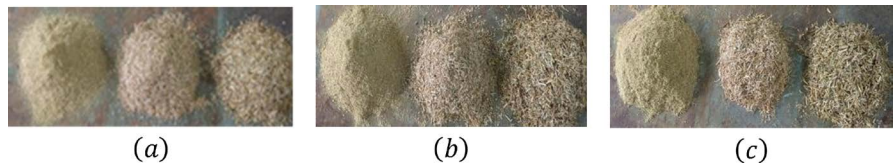


Figure 3. Presentation of the different aggregates by size and by zone after sieving; (a) peripheral zone, (b) intermediate zone, (c) central zone.

Table 1. Different densities of constituents.

Element	Plaster	Raffia			References
		Periphery	Intermediate	Center	
ρ (kg/m ³)	650	28,183	143,929	121,496	[28]

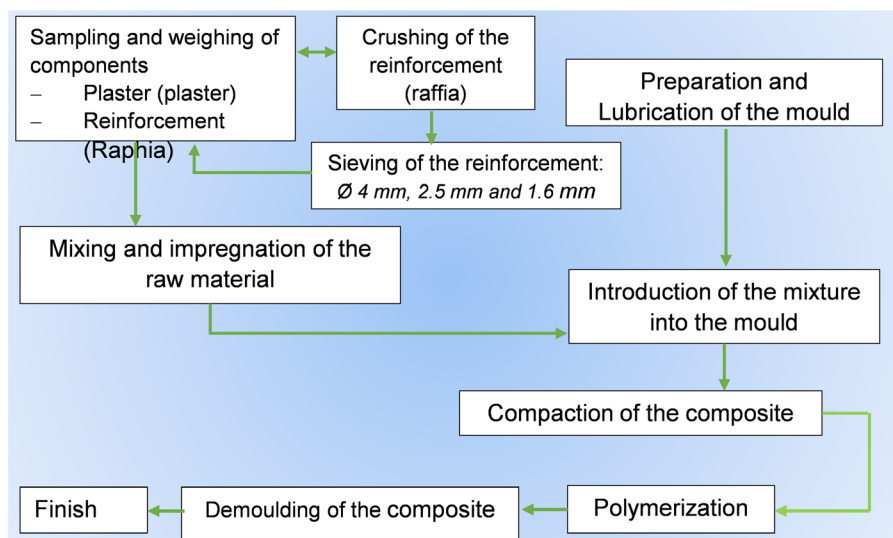


Figure 4. Main stages of the contact molding process.

The different formulations are presented in **Table 2**. It contains the volume ratios of plaster and reinforcement from the peripheral zone. To perform the combinations of the samples, a relationship was established between the densities and the useful volume of the cubic dimension mold ($180 \times 180 \times 10$ mm) and the quantities are summarized in **Table 2**.

The samples are made according to the mass of each zone and with a ratio of water and plaster ($w/p = 1$) for semi-hydrated β plaster [29]. Considering the combinations of **Table 2**, the shaping of the composites is done as follows:

- Impregnation of the reinforcement with the matrix;
- Shaping to the cubic geometry of the mould;
- Hardening of the mixture.

The manufacture of the specimens required the use of the materials shown in **Figure 5** and the water used for the mixing the plaster compounds was drinking water.

The mixing procedure is done according to standard and summarize in **Table 3**.

After mixing, the composite is introduced in mold of size $180 \times 180 \times 10$ mm and kept during 25 min before demolding. These sizes are adapted to the experimental devices for the thermal conductivity measurements. A total of twenty-seven (27) samples were formulated, including nine (9) per zone for three

Table 2. Quantities of components by formulation and by size of raffia particles.

Particle size (mm)	Reinforcement rate (%)	Plaster rate (%)	Mass of reinforcements (g)	Plaster mass (g)	Designations	Sample numbers
$T \leq 1.6$	5	95	15.09	286.81	P11	3
	10	90	30.19	271.72	P12	
	15	85	45.28	256.62	P13	
$1.6 < T \leq 2.5$	5	95	15.09	286.81	P.21	3
	10	90	30.19	271.72	P22	
	15	85	45.28	256.62	P23	
$2.5 < T \leq 4$	5	95	15.09	286.81	P31	3
	10	90	30.19	271.72	P32	
	15	85	45.28	256.62	P33	

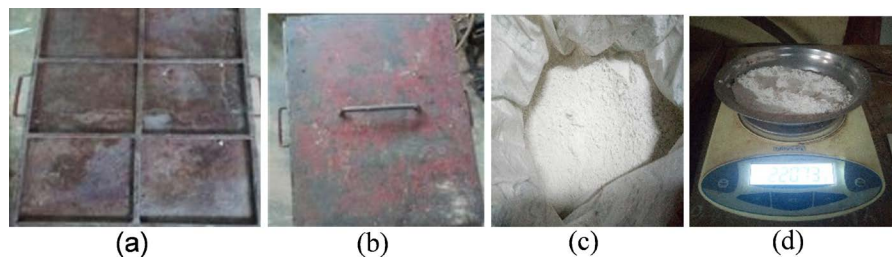
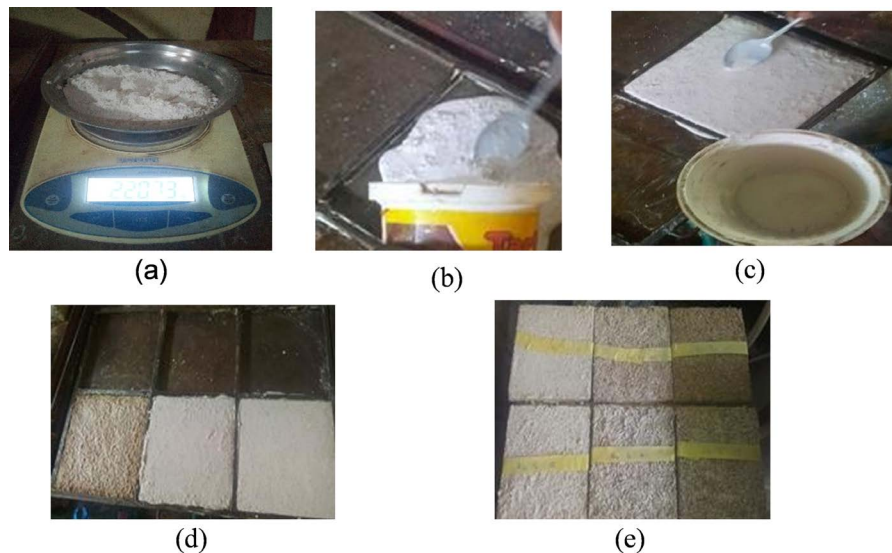


Figure 5. Materials used for the manufacture of the composite, (a, b) mould, (c) bag of 40 kg of plaster, (d) digital scale.

Table 3. Summary of the mixing procedure.

Working Time	2 min	30"	2 to 3 min
Addition	Raffia particles + plaster	-	Water
Mixing	Mixing	Rest	Mixing

**Figure 6.** Presentation of the main steps in the composite production of (a) weighing, (b) and (c) mixing and placing the mixture in the mold, (d) polymerization, (e) demolding and finishing.

(03) sizes of raffia *vinifera particles* (1.6 mm; 2.5 mm; 4 mm), three (03) percentages of reinforcement (5wt%, 10wt%, 15wt%) and three (03) unreinforced plaster samples. **Figure 6** shows the different steps in the process for obtaining the plaster and raffia *vinifera particles* based composite material. The sample are cured in an ambient condition and dried over a period of five to two weeks and subjected to physical, mechanical and thermal tests.

2.3. Characterization of Composite Materials and Specimens

2.3.1. Physical Properties

The optimization of the building's envelope parameters depends on several factors [1] including the construction materials properties. To do this, the physical properties of the new composite to be determined are: the apparent and real densities and the moisture absorption rate.

1) Bulk Density

The determination of the density (ρ_{ap}) is governed by the European standard EN 323, 1993 [30] and obtained by applying the following formulas (1) and (2):

$$\rho_{ap} = \frac{m}{V} \quad (1)$$

With:

- ρ_{ap} : bulk mass (g/cm^3).

- m : material mass,(g).
- V : the test specimen average volume (cm³).

$$V = L \times l \times e \quad (2)$$

where:

- V : average volume of the specimen (cm³);
- L : average length of the specimen (cm);
- l : average width of the specimen, (cm);
- e : Thickness of the specimen (cm).

2) The real density

The real density ($\rho_{réelle}$) is determined experimentally from the Archimedes' buoyancy principle and by applying the following formulas (3)-(6):

$$m_p = m_{e+p} - m_e \quad \text{or} \quad \rho_p = \frac{m_p}{V_p} \quad (3)$$

$$V_p = \frac{m_{e+p} - m_e}{\rho_p} \quad (4)$$

With:

- V_p : paraffin volume (cm³);
- ρ_p : paraffin density(g/cm³);
- m_{e+p} : mass of the waxed specimen (g);
- m_e : specimen mass (g).

$$V_e = V_f - (V_i + V_p) \quad (5)$$

With:

- V_e : volume of the specimen (cm³);
- V_f : final volume(cm³);
- V_i : initial volume (cm³);
- V_p : volume of paraffin (cm³).

$$\rho_{real} = \frac{m_e}{V_e} \quad (6)$$

where:

- ρ_{real} : real density (g/cm³);
- m_e : mass of the specimen (g);
- V_e : volume of the specimen (cm³).

3) Moisture absorption rate

The determination of the moisture absorption rate is conducted in accordance with the European standard EN 317, 1993 [31] and obtained by the following formula (7):

$$\omega_h \% = \frac{m_i - m_f}{m_i} \times 100 \quad (7)$$

With:

- ω_h : moisture absorption rate (%);

- m_i : initial mass of the sample (g);
- m_f : final mass of the sample(g).

2.3.2. Thermal Properties

The thermal characterization of the composite material relates to the thermal conductivity (λ), the thermal diffusivity (a), the thermal effusivity (E), the volumetric heat capacity (C_v) by the method of the asymmetric hot plane [32] in accordance with the ASTM D5930-97 standard method.

This method, whose principle is represented in **Figure 7**, comprises a flat section heating element ($10\text{ cm} \times 10\text{ cm}$) on which a sample of the same section is placed. On either side of the heating plate and the sample, are superimposed a polystyrene block and an aluminum block of 4 cm of thickness. A thermocouple consisting of two wires of diameter ($\phi \leq 0.05\text{ mm}$) and placed on the faces of the sample. The thermocouple being in contact with a deformable medium, its presence does not generate additional contact resistance. Also, polystyrene being an insulator, the contact resistance between the heating element and the polystyrene can be neglected.

A similar device has been used in previous studies [32] [33] [34]. The assumption is that the samples are considered as semi-infinite media and the transfer is unidirectional ($1D$) in the center of the heating resistor and the sample. Considering the very low heat flux value reaching the aluminum blocks through the polystyrene and their high capacity, their temperature is assumed to be equal and constant. The method is transient, a constant heat flux step is applied to the heating resistor on the front face of the sample for a certain time (typically 2 min) and the measurements of the temperature $T(t)$ evolution are recorded for about 10 minutes. In these hypotheses, we can write and by applying the quadrupoles formalism, on the device represented by **Figure 7**. By modelling this heat transfer, we can calculate the change in temperature at the center of the sample. Modelling using the quadrupole method and applying Sthefest's method,

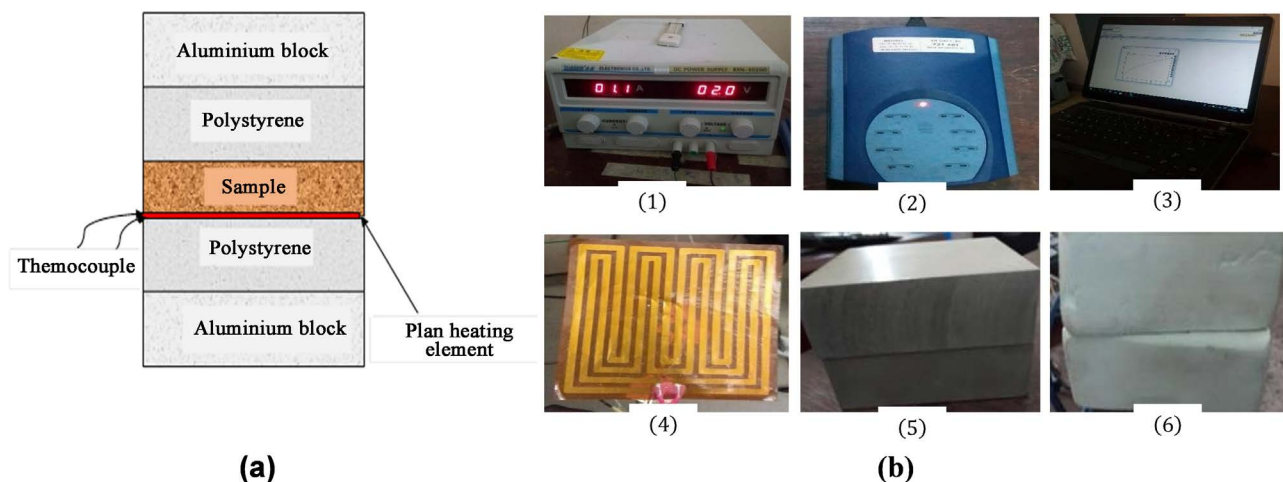


Figure 7. Plan view of the hot plane method (a) experimental Principle and (b) experimental device with (1) heating source (2) Pickolog, (3) laptop, (4) heating plate, (5) aluminum block and (6) polystyrene Block.

for a semi-infinite medium, the temperature difference $T(t) - T(0)$ can be calculated using the Equation (8) below [34]:

$$T(t) - T(0) = \frac{\phi_0}{2} \left[R_{com} - \frac{m_c}{2(ES)^2} \right] + \frac{\phi_0}{ES\sqrt{\pi}} \sqrt{t} \quad (8)$$

where:

- $T(0)$, the temperature initial time (in K);
- $T(t)$, the temperature at time t (in K);
- ϕ_0 , the initial heat flow set (in $W \cdot m^2$);
- R_{com} the contact resistor (in $W \cdot m^2 \cdot K^{-1}$);
- m_c , the heat capacity of the thermocouple (in $J \cdot K^{-1}$);
- E , the thermal effusivity of the material sample (in $(J/m^2 \cdot K \cdot s^{1/2})$);
- S , the mean value of the sample section (in m^2);
- T , the measurement time (in s).

In a permanent state, the temperature difference between the different surfaces does not vary. The thermal conductivity (λ) can then be estimated using the formula (9) below:

$$\lambda = \frac{\phi_0 e}{S \Delta T} \quad (9)$$

With:

- λ , thermal conductivity (in $w/m \cdot k$);
- ϕ_0 , the initial density of heat flow set (in $W \cdot m^2$);
- e , the thickness of the sample (in m);
- S , the section of the sample (in m);
- ΔT , the temperature difference (in $^{\circ}K$).

From above equation it deduced the thermal diffusivity (α) [35] and the volumetric thermal capacity ($Cp = \rho c$) [36] by the following Equation (10) and (11):

$$E = \sqrt{\lambda \rho c} \quad (10)$$

With ρc , the volumetric thermal capacity of the material (in J/kg)

$$\alpha = \frac{\lambda}{\rho c} \quad (11)$$

With α the thermal diffusivity (in m^2/s).

2.3.3. Mechanical Characterization

A three-point bending moment test is obtained for the composite samples ($4 \times 4 \times 16 \text{ cm}^3$). The testing machine presented in **Figure 8** functions as a spring of stiffness $K = 301N$ is used for determining the load, the displacement and the flexural stress for each specimen at all applied forces. The flexural stress (σ_f) is calculated following Equation (12):

$$\sigma_f = \frac{3FL}{2bd^2} \quad (12)$$

where:

- F : Flexural load applied (N);
- L : Span (mm);
- b : Width of the sample (mm);
- d : thickness of the sample (mm).

The specimen is placed at the level of two supports distant of $L = 10$ cm. The Load F at the fracture point and the displacement of the specimen are reported. The test method follows the NF P 18-411 [37] standard flexural testing and according to the European standard 12089 [38].

Modulus of Rupture (MOR) was calculated according to RILEM TFR1 [39] using equation 12 which is applied by A. Salas-Ruiz *et al.* [40].

2.4. Experimental Study of the Habitable Cell Thermal Behavior

The experimental study focuses on the influence of the new thermal insulating composite material on the thermal behavior of a habitable cell.

2.4.1. Application Support

The support of the study is a habitable cell represented in **Figure 9**, with the following's characteristics:

- Manufacture of two living cell models of dimensions 20 cm \times 25 cm in Ayous wood panel of thickness 10 cm;
- Manufacture and installation of 10 cm thick plates of the new *raffia vinifera* particle and plaster based composite material on each wall of one of the living cells, as interior insulation.

2.4.2. Assumptions and Experimental Protocol

The study consists of two experiments conducted according to the synoptic of **Figure 10** and with the following hypotheses:

- Hypothesis 1 for experiment 1: the environment is conditioned at a temperature ranging from 22°C to 25.8°C to simulate a cold temperature in the



Figure 8. Equipment for test performing.

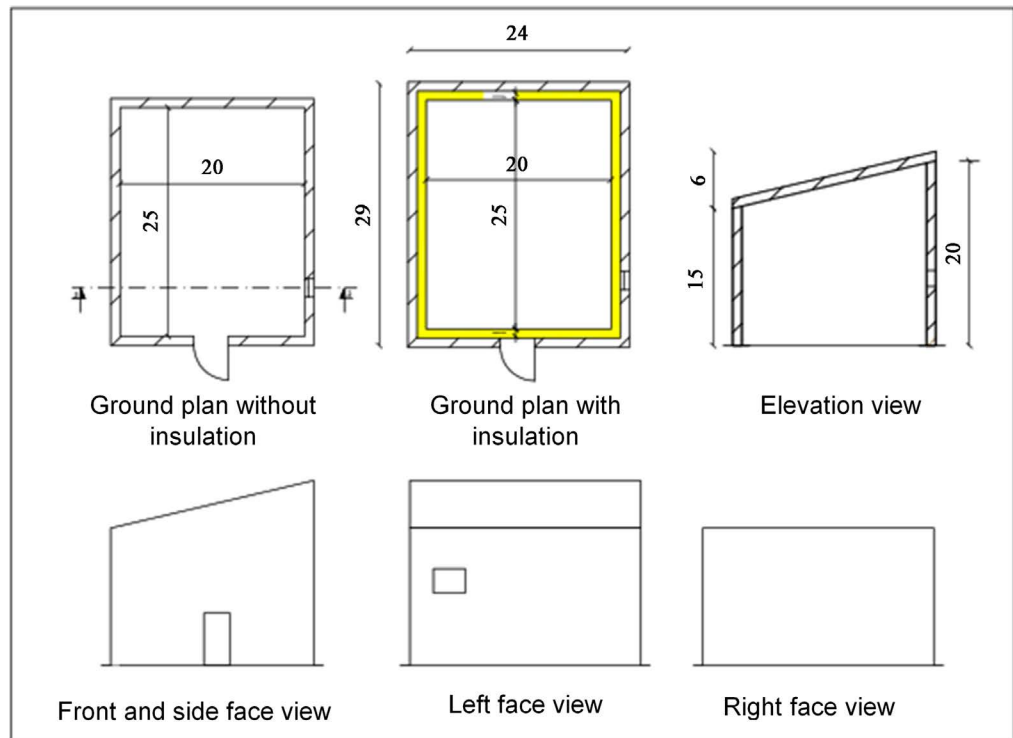


Figure 9. Plan of the habitable cell.

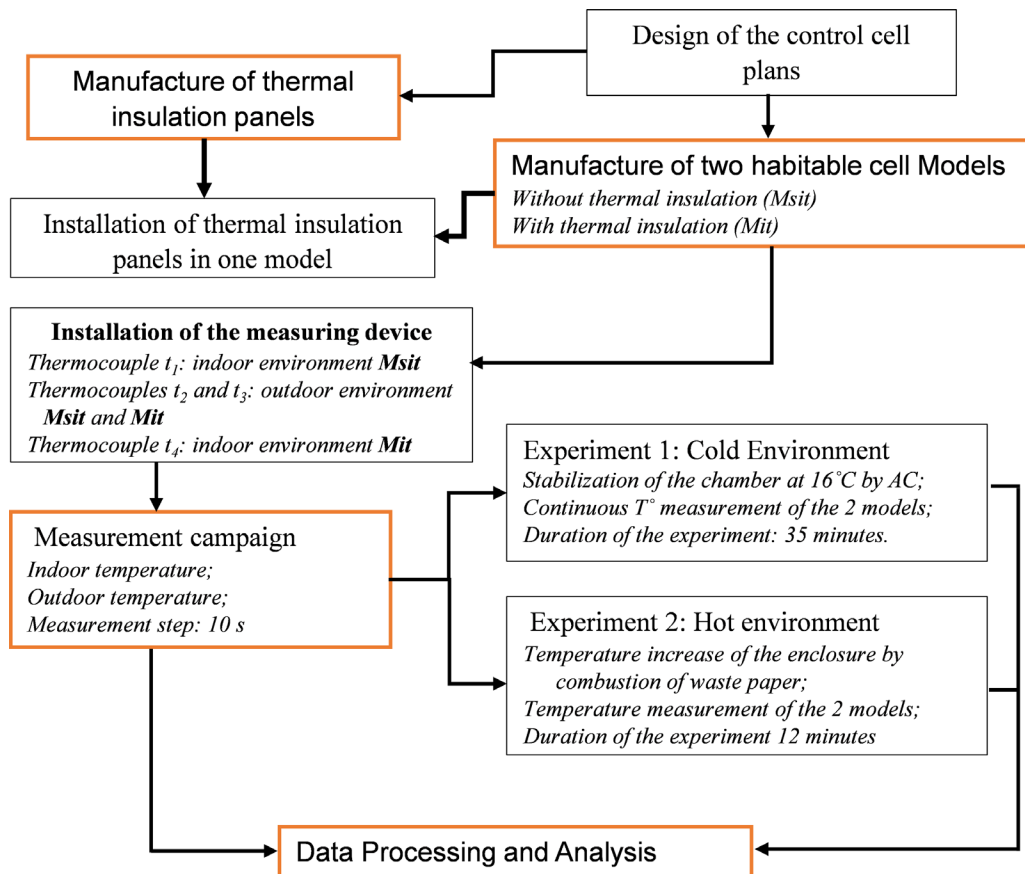


Figure 10. Synoptic of the habitable cell thermal behavior experimental study.

study area;

- Hypothesis 2 for experiment 2: the medium is conditioned at a temperature ranging from 28.4°C to 33.95°C to simulate a hot period in the study area.

2.4.3. Experimental Equipment

Figure 11 shows the two identical models of the habitable cell and the arrangements of the temperature measurement equipment as follows:

- The two models (with and without thermal insulation) are placed simultaneously in each enclosure;
- A thermocouple ($T_{i,Mn}$) for indoor room temperature of the model without insulation;
- A thermocouple ($T_{i,Mi}$) for indoor room temperature of the model with insulation;
- Two thermocouples (t_2) and (t_3) for the outside temperature (T_{ext}) of the models;
- The instrumentation of the models is made until the stabilization of the temperatures.

3. Results and Discussion

3.1. Characterization of Formulated Composite

3.1.1. Physical Properties

1) Densities

Figure 12 and **Figure 13** illustrate respectively the results obtained for apparent and real densities a function of reinforcement rate, zone and particle size of the samples.

The apparent and real density values obtained vary respectively between 604.57 ± 26.72 to 768.38 ± 14.67 kg/m³ and between 507.28 ± 111.85 to $634.35 \pm$

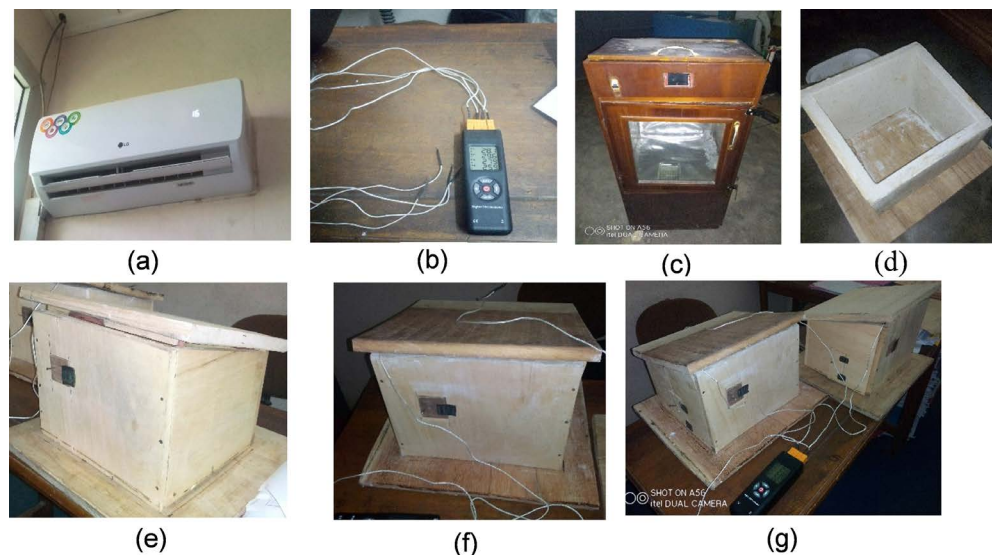


Figure 11. Experimental device; (a) air conditioner, (b) thermocouple, (c) enclosure, (d) insulated house interior view, (e) uninsulated house, (f) insulated house, (g) start of experiment.

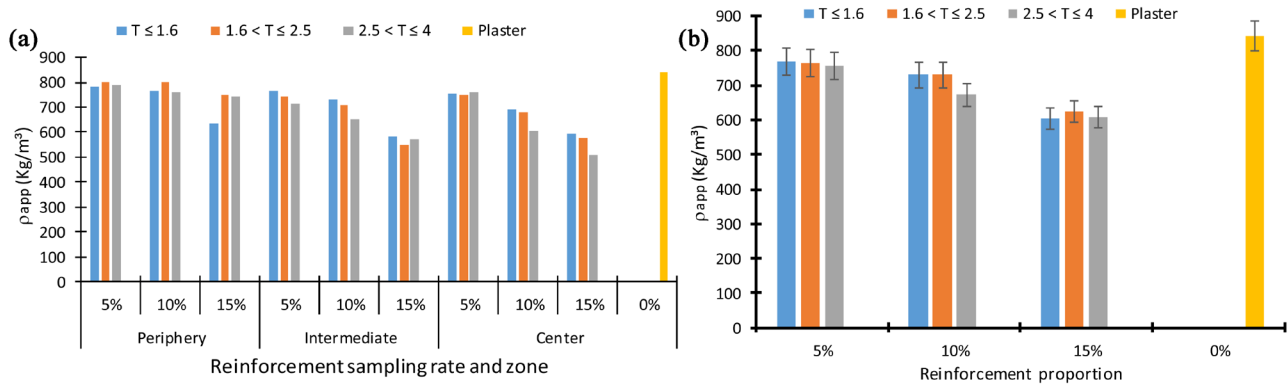


Figure 12. Evolution of the apparent density of the composite and the plaster (a) function of the rate and of the removal zone of the reinforcement (b) function of the rate of reinforcement.

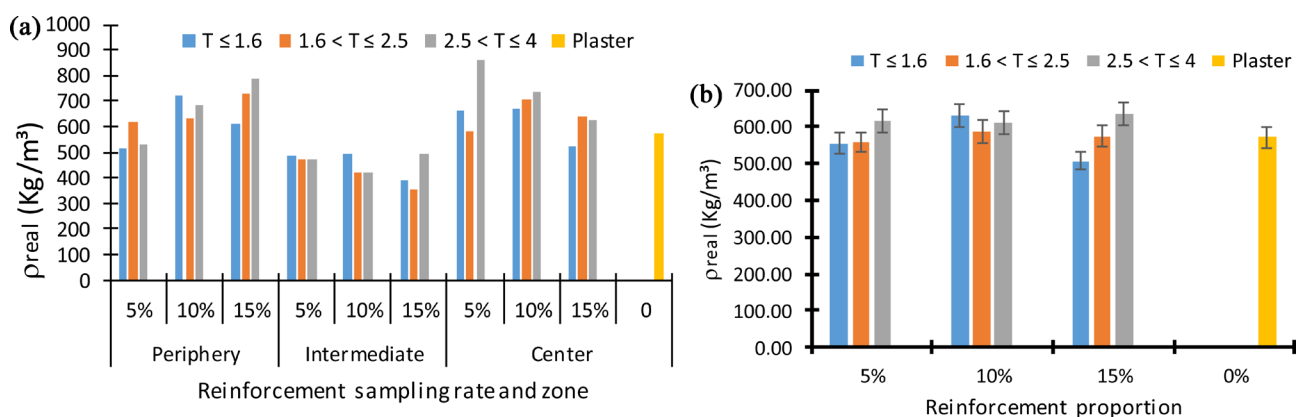


Figure 13. Evolution of the real density of the composite and of the plaster (a) function of the rate and of the removal zone of the reinforcement (b) function of the rate of reinforcement.

141.47 kg/m³ and correspond to a medium density material according to American standard ANSI A208 [41]. The accuracy in measuring density is evaluate par Standard deviation method. The density decreases progressively as the amount of the raffia vinifera in the composites samples increases. Similar effects were observed in others investigations [42].

2) Water absorption

Figure 14(a) and **Figure 14(b)** show the evolution of the water absorption rate as a function of the reinforcement rate and the particle size for the composite and the plaster.

The presence of pores in the bamboo particles of raffia *vinifera* and in the plaster also confers this property to the plaster matrix reinforced composite samples. In fact, when the composite is immersed in water, these voids absorb water by capillarity action and this quantity of water increases with the immersion time. The moisture absorption rate values obtained after 24 hours of immersion in water vary from $0.26\% \pm 0.08\%$ to $0.57\% \pm 0.11\%$. These results are significantly below than that of S. Manjit and C. Mridul, who observed for plaster reinforced with sisal fibres an absorption rate after 24 hours of immersion of 1.50% [43]. This difference may be due to the difference in proportion, rein-

forcement size and dimensions of the specimens used. And this could affect the thermal conductivity of an insulating material [44].

3.1.2. Thermal Properties

The tests carried out in the laboratory allowed us to determine the following thermal properties: thermal conductivity, thermal diffusivity, thermal effusivity and volumetric heat capacity. The evolution of these thermal parameters as a function of the size and the rate of reinforcements of the composite different formulations and the plaster is presented in **Figure 15** and **Figure 16**.

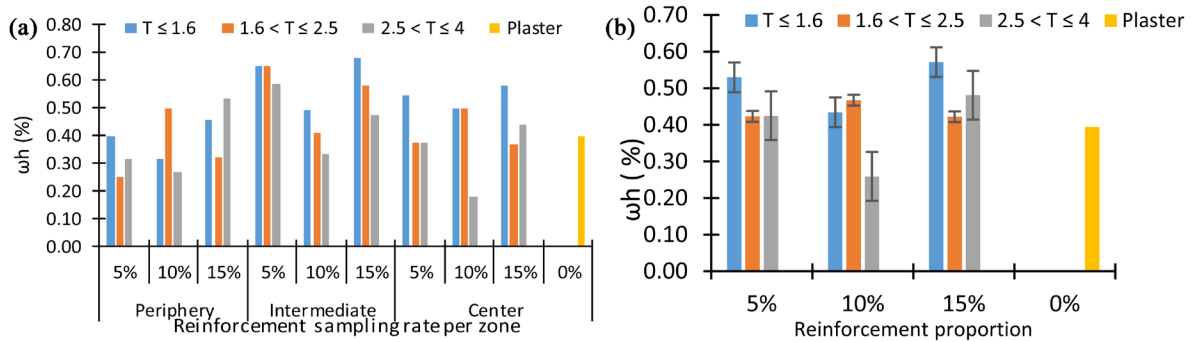


Figure 14. Evolution of the humidity absorption rate of the composite and the plaster (a) according to the zone and the reinforcement rate (b) according to the reinforcement rate.

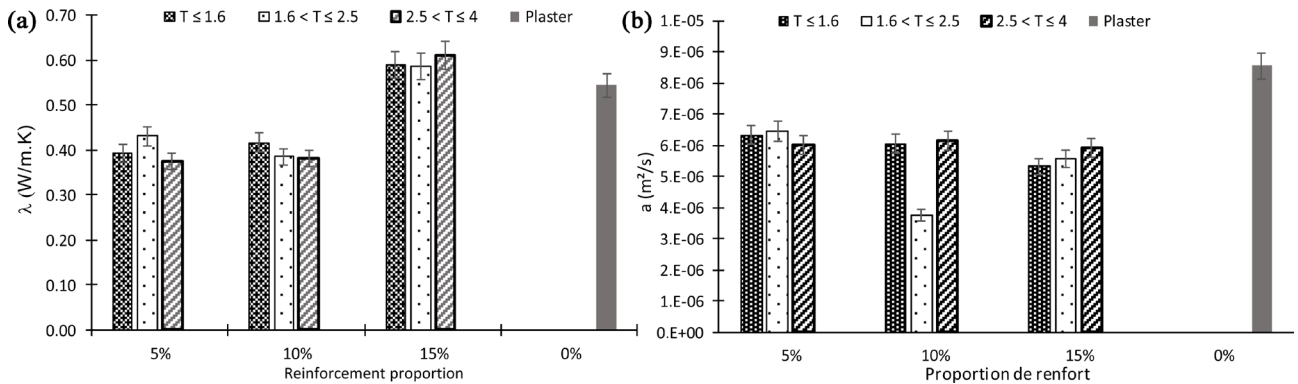


Figure 15. Thermal properties for the different composite and the plaster (a) Thermal conductivity and (b) Thermal diffusivity.

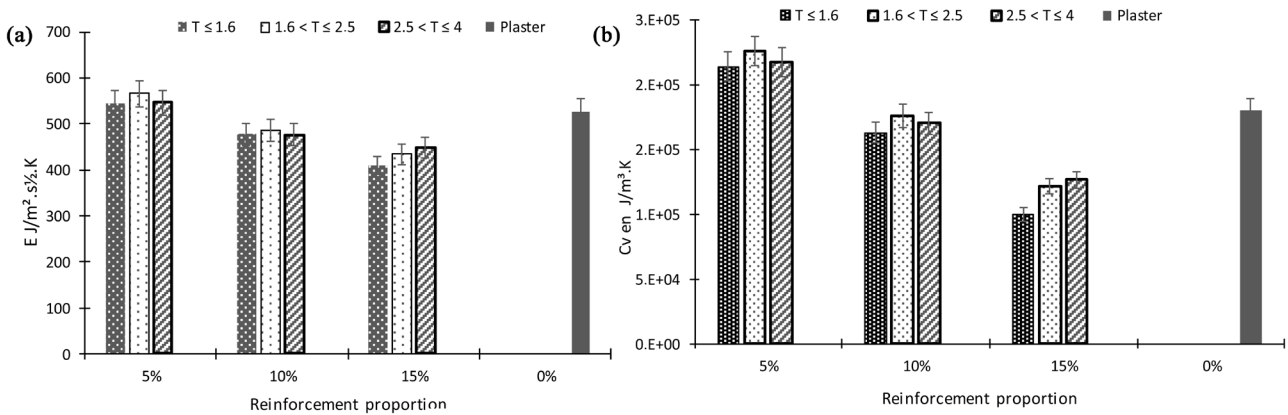


Figure 16. Thermal properties for the different composite and the plaster (a) Thermal effusivity and (b) Volumetric heat capacity.

The thermal conductivity values of the raffia vinifera particles and plaster based composite material range from 0.38 ± 0.11 to 0.61 ± 0.21 W/m·K. It is noted that the thermal conductivity of the composite is lower than that of the unreinforced plaster at 0.54 W/m·K. This positive effect of the fibres incorporated in plaster composites are also mentioned in other previous study [45]. As for the thermal diffusivity, it is between $3.8 \times 10^{-6} \pm 1.3 \times 10^{-6}$ à $6.5 \times 10^{-6} \pm 1.1 \times 10^{-6}$ (m²/s) and that of the unreinforced plaster and of $8.6 \times 10^{-6} \pm 2.1 \times 10^{-7}$ (m²/s); the lowest value of diffusivity is observed for the reinforced plaster. This difference in result may be due to the nature, the zone and the proportions of reinforcement used. Regarding the thermal effusivity of the composite, it varies from 409.34 ± 25.74 à 565.68 ± 59.07 (J/m²·S^{1/2}·K) and that of the unreinforced plaster 527.58 ± 9.30 (J/m²·S^{1/2}·K); the capacity to slow down, to stabilize the heat flow of the composite is more important than that of the unreinforced plaster. In addition, the composite material's thermal capacity range from $1.0 \times 10^5 \pm 2.2 \times 10^4$ à $2.3 \times 10^5 \pm 5.0 \times 10^4$ (J/m³·K) and that of the unreinforced plaster from $1.8 \times 10^5 \pm 1.6 \times 10^3$ (J/m³·K), so the capacity of the unreinforced plaster to storing heat is greater than that of reinforced plaster. From the above, it can be deduced that the presence of reinforcement by *raffia particles* in plaster increases the composite material thermal insulation capacities which is in accordance with the results obtained by Saad Azzem, L. and Bellel, N. [15] [45]. However, there is a drop in the average thermal diffusivity value in case of 10wt% reinforcement for the size between 1.6 and 2.5 mm. This is linked to the density of the particles sampled in the intermediate and central zones, the quantity of particles in the mix and their low thermal diffusivity between individual samples.

3.1.3. Mechanical Property

A three-point bending test is done for specimen inertia $I = 2.13 \times 10^{-7}$ (m⁴) of composite insulating material samples. All the flexural strength is presented in **Figure 17** for the different samples. Almost all the results are below the minimum set by the standard [46], except the composite at 5wt% of reinforcement rate by raffia size between 2.5 and 4.0 mm which increase of 37.03%. The best results are 0.87 and 1.01 MPa at 5wt% reinforcement with respectively sizes between 1.6 and 2.5 mm and between 2.5 and 4.0 mm and 0.854 MPa at 15wt% reinforcement of raffia size lower than 1.6 mm. For these samples, there is an increase the flexural strength from 15.97% to 37.03% and its function of both the particles size, the percentage of reinforcement and the specimen density or degree of pressing the specimen as obtained by M. Ali *et al.* [18]. These effects were observed by A. Zaragozaenzal *et al.*, who indicated that the increase of the flexural strength is more than 20% for the composite with fibres, compared to composite lightened without fibres [45].

3.2. Simulation Results for the Habitable Cell Thermal Behavior

On reminder, $T_{i,Mn}$ and $T_{i,Mi}$ are defined as the internal temperature respectively of the non-insulated enclosure, and of the insulated enclosure and T_{ext} the aver-

age temperature of the external environment.

3.2.1. Thermal Behavior in a Cold Environment

Figure 18 reports the results obtained for the variations of the exterior and interior temperatures of each model studied.

The outside temperature T_{ext} decreases under the effect of air conditioning set at 16°C. The temperature values T_{ext} fluctuate between 22.3°C and 25.8°C during the instrumentation. From 0 to 400 s, the temperatures $T_{i,Mn}$ and $T_{i,Mi}$ evolves in phase, they vary between 27.4°C and 28°C. After a certain time, we record peaks in the curve $T_{i,Mn}$, these peaks may be due to the exchange of air between the interior and exterior environment through the thermal bridges thus influencing the internal temperature of the house. In the same way the temperature $T_{i,Mi}$ is almost linear, it is almost constant while $T_{i,Mn}$ varies; which indicates that the

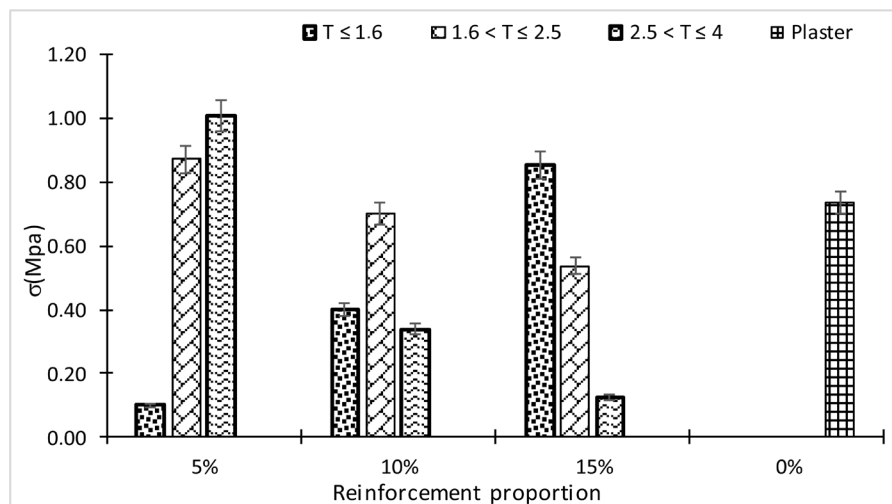


Figure 17. Flexural stress in bending of each composite and plaster.

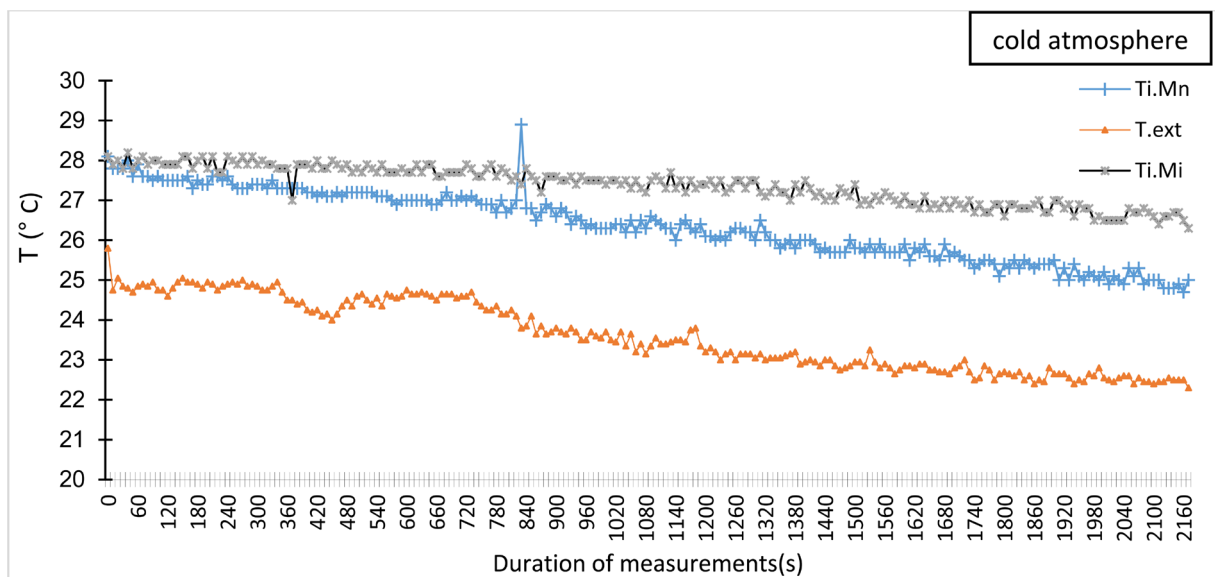


Figure 18. Evolution of the outside and inside temperatures of the two habitable cells in a cold environment.

wood material is more heat-conducting than the raffia vinifera particles and plaster based composite material. At the end of this experiment, it results a temperature damping of 4°C and 1°C in the insulated house interior environment respectively in comparison to the outside environment and the uninsulated house interior environment.

3.2.2. Thermal Behavior in Hot Environment

Figure 18 and **Figure 19** show the different variations of external and internal temperatures during the habitable cell thermal instrumentation.

From the experiment beginning, it appeared that the temperatures $T_{i,Mn}$ and T_{ext} are substantially equal, and they range from 28.4°C and 30.8°C. After 60 seconds, the insulated house indoor temperature $T_{i,Mi}$ is almost static: this justifies the effectiveness of the new insulating composite material made with plaster and raffia particle (*C95P5R*) to regulate the heat transfer between the hot external environment and the habitable cell internal environment, while at 210 s the indoor and outdoor temperatures $T_{i,Mn}$ and T_{ext} follow approximately the same evolution. This behavior can be justified by the low capacity of the wood material in the presence of heat. At the end of the experiment, there is a temperature difference of approximately 4°C between the insulated house and the outside environment and of 5.8°C between the uninsulated house and the insulated one. This gap shows a good thermal insulation capacity of the raffia vinifera particles and plaster based composite material (*C95P5R*).

From these two experiments, the insulating capacity of the composite is more visible in the case of a hot external environment in that the difference in temperature between the uninsulated house and the insulated one is $\Delta T = 5.8^\circ\text{C}$ while the difference in temperature between the two houses for the cold external environment is $\Delta T = 1^\circ\text{C}$.

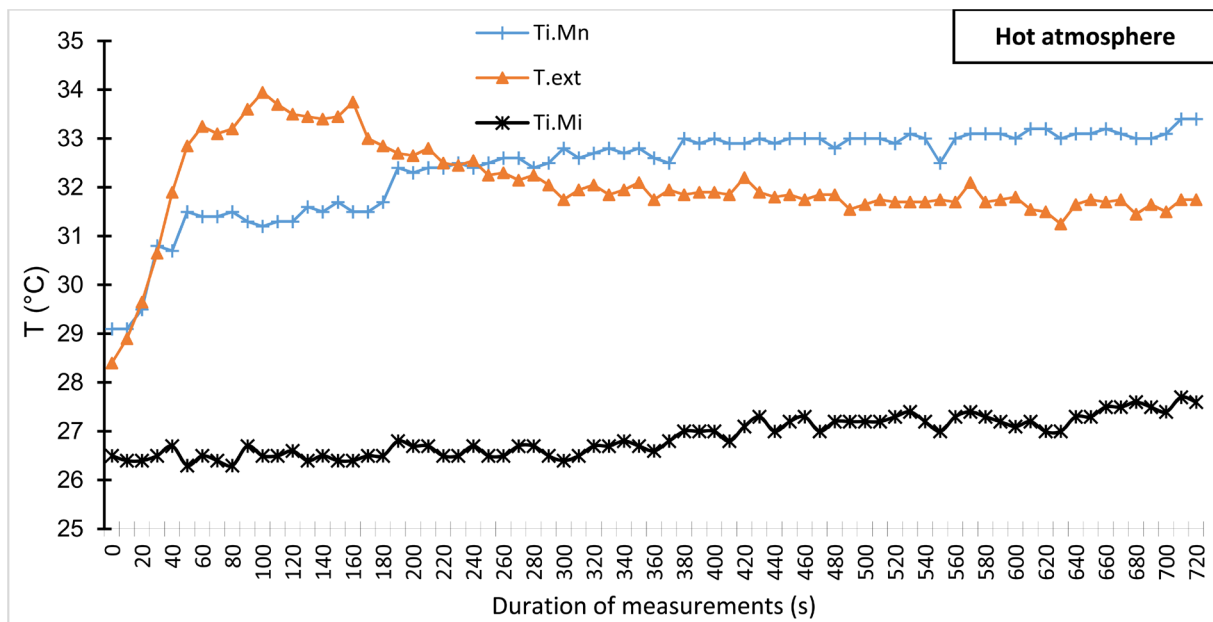


Figure 19. Evolution of the indoor and outdoor temperatures of the two habitable cells in a hot environment.

4. Discussion

4.1. Summary of Mains Finding

From the results obtained, it is observed that the raffia vinifera particles and plaster based composite materials densities are respectively proportional to the rate of reinforcement and to the size of the raffia particles in the composite. Regarding the moisture absorption rate, it is greater for the raffia vinifera particles and plaster-based composite compared to the plaster material.

- The apparent density value of the new composite samples for any size and substitution proportion of raffia vinifera particles is less (average 17,42%) than the plaster samples;
- The real density of the new composite is greater (+9.81%, +0.43% and +8.39%) than that of the plaster respectively for 10wt% incorporation for size less than 1.6 mm, 15wt% incorporation for size between 1.6 and 2.5 mm and for any incorporation proportion of raffia vinifera particles reinforcement of size between 2.5 and 4.0 mm;
- The new composite absorbs more moisture (+13.13%) than the plaster samples except at 10wt% reinforcement rate of the raffia vinifera particles size of $2.5 < T \leq 4$ mm for center zone. This effect was observed with date palm fibres [13].

This variation in density is a function of the rate and the size of the reinforcement in the composite and the bulk density has an inverse relationship with the percentage of natural fibres [15]. This effect is due to the difference in mass, moisture content and particle distribution in the composite according to L. Vidil [47].

On the thermal level we record an increasing in the value of the thermal conductivity at the maximum proportion of reinforcement while the diffusivity and the thermal effusivity are maximum at the minimum proportion of reinforcement. As for the volumetric thermal capacity, it increases for a minimum reinforcement size and is lower than that of unreinforced plaster.

- The thermal conductivity of the composite at 5wt% and 10wt% raffia incorporation rate of any size studied is less than that of unreinforced plaster;
- At all percentage of incorporation, the RVP size has a small influence on the thermal conductivity and the difference is 0.02 to 0.05 W/m·K;
- For the different size, the thermal conductivity variation is large between the raffia vinifera reinforcement rate of 5wt% and 15wt%, 10wt% and 15wt%, but small between the raffia vinifera reinforcement rate of 5wt% and 10wt%;
- The composite thermal diffusivity is lower than that of the unreinforced plaster sample for the raffia vinifera different size and incorporation rate studied. However, there is a minimum asymptote of thermal diffusivity of the composite at 10wt% of incorporation rate of raffia vinifera size between 1.6 and 2.5 mm;
- The new composites based on 10wt% and 15wt% incorporation rate of raffia vinifera of different size studied has a lower thermal effusivity than the plas-

ter samples and inversely at 5wt% of reinforcement rate. So, the composite thermal effusivity is inversely proportional to the incorporation rate and a small influence of the raffia vinifera size studied;

- The thermal capacity of the new composites based on 5wt% reinforcement rate of raffia vinifera different size studied is higher than that of the unreinforced plaster samples and inversely for the samples at 10wt% and 15wt% reinforcement rate.

Moreover, the bending stress increases with the presence of reinforcement. Indeed, the flexural strength is superior to that of unreinforced plaster for composites based on 5wt% raffia of size superior to 1.6 mm on the one side and 15wt% raffia reinforcement of size inferior to 1.6 mm on the other. Similar outcomes were obtained by [48]. This result shows that we can proceed to rely on the raffia vinifera size and reinforcement rate to improve the tensile strength of the new composite. In addition, it can be seen that the size of 1.6 mm is a bottom limit and therefore a reference particle size on which we can base the formulation of the composite by adjusting the rate of reinforcement as a variable. And the less a material is dense, the more it contains air-filled voids between the particles, the lower the thermal conductivity, reflecting a greater thermal capacity. It is found that, depending on the particles size and rate, the *raffia vinifera fiber* reinforces the composite's ability to resist bending, which agrees with the result on the mixture of coconut particles and fibres with the plaster by D. Kumar *et al.* [49]. These values are more interesting than the results obtained for a composition of plaster + rice husk of inertia $I = 5.51 \times 10^{-7} \text{ m}^4$ with a flexural stress of 0.359 MPa [50] and $0.3 \pm 0.04 \text{ MPa}$ for specimens of size $(40 \times 40 \times 29) \text{ mm}^3$ reinforced with non-oriented fiber of *Rhectophyllum Camerunense* (RC) for a reinforcement percentage of 3.35% [51].

Finally, these results indicate that the thermal properties of the raffia vinifera particles and plaster based composite material are influenced according to the incorporation rate and the maximum particle size of the stabilizer used. In other similar studies, the materials incorporated modify the thermal conductivity of the resulting materials depending on the quantity, the volume fraction and properties [14] [36]. It appears that the best composition as a thermal insulator is reinforced plaster by *raffia vinifera particles* at a 5wt% rate and size between 2.5 and 4.0mm. This composite has the best ratio of thermo-physical-mechanical properties, which are summarized in **Table 4**.

For the habitable cell model thermal behavior instrumentation, this composite 95wt% plaster + 5wt% *raffia vinifera particles* (C95P5R), is used as the building

Table 4. Properties of the best raffia vinifera particles and plaster-based composite.

Composite	ρ_{app} (g/cm ³)	ρ_{real} (g/cm ³)	ω_h (%)	λ (W/m·K)	a (m ² /s)	E (J/m ² ·S ^{1/2} ·K)	C_p (J/m ³ ·K)	σ_f (MPa)
95 Plaster + 5wt% raffia vinifera particles	755.81	617.90	0.42%	0.38	6×10^{-6}	546.16	2×10^5	1.01

envelope's thermal insulation material. At the end of this experiment, it results a temperature damping of 4°C and 5.8°C in the insulated house interior environment respectively for cold and hot cases in comparison to the outside environment and the uninsulated house interior environment, within the uncertainty range of the data logger is $\pm 1.7^\circ\text{C}$.

4.2. Strengths and Limitations

A new composite as thermal insulation material that integrates an agricultural and industrial secondary resource is developed. Then, we formulated and determined the *plaster and raffia vinifera* based composite material physical, thermal and mechanical properties and compared to unreinforced plaster properties.

- The good thermal properties of the plaster-raffia vinifera composite is encouraging in their used for building envelopes thermal insulation;
- The innovated by simultaneous assessment of the sampling area, the particle size and the reinforcement rate of the raffia vinifera in the composite study;

This study brings a substantial contribution to the valorization of the local resources in sustainable construction but the context was marked by constraints such as:

- The sample cure is down in laboratory conditions that are not identical to their real and natural conditions of use;
- The rapid hardening of the mixture of plaster and raffia vinifera;
- The specimen's curing time was short, 12 days maximum before testing;
- The habitable cell model had a small size and far from real housing dimensions, like single storage habitat.

4.3. Implications on Practice and Research

The study's results show the possible used of plaster and raffia vinifera at precise rate and size to obtain a thermal insulation composite eco-material.

Further experimental research is recommended in order to study more:

- The physical and mechanical properties such as fire resistance, compressive strength, stress test;
- The behavior of habitable cell made with other local material such as earth based material and cement block;
- The study of economic profitability of the new composite material compared to the existing insulators.

To do this, it's important to let the samples dry for a longer period of time in order to observe again the behavior of the material and to note the possible variations.

5. Conclusions

In the present work, composites were developed by plaster with raffia vinifera particles (RVP) using different size. The effects of four different (RVP) incorporation (*i.e.*, 0wt%, 5wt%; 10wt%; 15wt%) on physical (density and water absorp-

tion), thermal properties, mechanical strength of the composites were investigated. In addition, the use of the raffia vinifera particles and plaster based composite material as building envelopes thermal insulation material is studied by the habitable cell thermal behavior instrumentation in hot and cold environment conditions. The results indicate that the incorporation raffia vinifera particle leads to improve the new composite physical, mechanical and thermal properties. And the parametric analysis reveals that the sampling rate and the size of raffia vinifera particles are the most decisive factor to impact these properties, and to decreases in the thermal conductivity which leads to an improvement to the thermal resistance and energy savings. The best improvement of plaster composite was achieved at the RVP loading of 5wt% and size between 2.5 and 4.0 mm (C95P5R) which were about 0.376 W/m·K (30.98% higher than the plaster sample). The water absorption test shows that the water absorption rate is higher compared to plaster samples except at the RVP loading of 10wt% of size between 2.5 and 4.0 mm and depends on the RVP size and the incorporation rate. Afterward, the flexural test showed the flexural strength of samples increase compared to that of the plaster with the maximum improvement was obtained at the RVP loading of 5wt% and size between 2.5 and 4.0 mm, which was about 1.01 MPa (37.06% higher than the plaster sample). Additionally, the habitable cell experimental thermal behavior, with the new raffia vinifera particles and plaster-based composite as thermal insulating material for building walls, gives an average damping of 4°C and 5.8°C in the insulated house interior environment respectively for cold and hot cases in comparison to the outside environment and the uninsulated house interior environment, within the uncertainty range of the data logger is $\pm 1.7^\circ\text{C}$.

In conclusion, the studied highlight that the new raffia vinifera particles and plaster based composite material are suitable as thermal insulation in building and the best composite is obtained at the raffia vinifera particles size between 2.5 and 4.0 mm loading of 5wt% and with a good ratio of thermo-physical-mechanical properties. This mixture gives the new composite thermal insulation properties applicable in the eco-construction of habitats in tropical environments.

Author Contributions

“Conceptualization and methodology, E. M. and D.T.; drawing software, D.T.; validation, EM., K.I. and D.T.; formal analysis, E.M. and D.T.; investigation, D.T.; resources and data curation, D.T. and A.O.; writing—original draft preparation, E.M. D.T. and K.I.; writing—review and editing, E.M.; visualization, E.M and K.I.; supervision, D.T. and S.K. All authors have read and agreed to the published version of the manuscript.”

Declaration of Competing Interest

The authors declare that they have no known competing financial interests or personal relationships that could have appeared to influence the work reported

in this paper.

Data Availability

Data will be made available on request.

Conflicts of Interest

The authors declare no conflicts of interest regarding the publication of this paper.

References

- [1] Kumar, D., Alam, M., Memon, R.A. and Bhayo, B.A. (2022) A Critical Review for Formulation and Conceptualization of an Ideal Building Envelope and Novel Sustainability Framework for Building Applications. *Cleaner Engineering and Technology*, **11**, Article ID: 100555. <https://doi.org/10.1016/j.clet.2022.100555>
- [2] UNEP (2020) Global Status Report for Buildings and Construction. Nairobi.
- [3] Losini, E.A., Grillet, A.-C., Woloszyn, M., Lavrik, L., Moletti, C., Dotelli, G. and Caruso, M. (2022) Mechanical and Microstructural Characterization of Rammed Earth Stabilized with Five Biopolymers. *Materials*, **15**, Article No. 3136. <https://doi.org/10.3390/ma15093136>
- [4] Ali, M., Almuzaiqer, R., Al-Salem, K., Alabdulkarem, A. and Nuhait, A. (2021) New Novel Thermal Insulation and Sound-Absorbing Materials from Discarded Face-masks of COVID-19 Pandemic. *Scientific Reports*, **11**, Article No. 23240. <https://doi.org/10.1038/s41598-021-02744-8>
- [5] Al-Salem, K., Ali, M., Almuzaiqer, R., Al-Suhaibani, Z. and Nuhait, A. (2023) Recycling Discarded Facemasks of COVID-19 Pandemic to New Novel Composite Thermal Insulation and Sound-Absorbing Materials. *Sustainability*, **15**, Article No. 1475. <https://doi.org/10.3390/su15021475>
- [6] Neri, M. (2022) Thermal and Acoustic Characterization of Innovative and Unconventional Panels Made of Reused Materials. *Atmosphere*, **13**, Article No. 1825. <https://doi.org/10.3390/atmos13111825>
- [7] Jedidi, M. and Abroug, A. (2020) Valorization of *Posidonia oceanica* Balls for the Manufacture of an Insulating and Ecological Material. *Jordan Journal of Civil Engineering*, **14**, 417-430.
- [8] Ali, M., Alabdulkarem, A., Nuhait, A., Al-Salem, K., Almuzaiqer, R., Bayaouq, O., Salah, H., Alsaggaf, A. and Algafr, Z. (2020) Thermal Analyses of Loose Agave, Wheat Straw Fibers and Agave/Wheat Straw as New Hybrid Thermal Insulating Materials for Buildings. *Journal of Natural Fibers*, **18**, 2173-2188. <https://doi.org/10.1080/15440478.2020.1724232>
- [9] Ali, M. (2016) Microstructure, Thermal Analysis and Acoustic Characteristics of *Calotropis procera* (Apple of Sodom) Fibers. *Journal of Natural Fibers*, **13**, 343-352. <https://doi.org/10.1080/15440478.2015.1029198>
- [10] Malbila, E., Delvoie, S., Toguyeni, D. and Courard, L. (2021) Improving the Building Energy Efficiency and Thermal Comfort through the Design of Walls in Compressed Earth Blocks of Agricultural and Biopolymer Residues Masonry. *Current Journal of Applied Science and Technology*, **40**, 7-22. <https://doi.org/10.9734/cjast/2021/v40i4531624>
- [11] EstÈVe, P., Beckett, C., Pedreschi, R., Bosche, F., Morel, J.C., Charef, R. and Habert,

- G. (2022) Developing an Integrated BIM/LCA Framework to Assess the Sustainability of Using Earthen Architecture. *IOP Conference Series Earth and Environmental Science*, **1078**, Article ID: 012100. <https://doi.org/10.1088/1755-1315/1078/1/012100>
- [12] Zhang, Z., Zhang, N., Yuan, Y., Phelan, P.E. and Attia, S. (2023) Thermal Performance Analysis of an Existing Building Heating Based on a Novel Active Phase Change Heater. *Energy & Buildings*, **62**, Article ID: 106912. <https://doi.org/10.1016/j.enbuild.2022.112646>
- [13] Augustia, V.A., Chafidz, A., Setyaningsih, L., Rizal, M., Kaavessina, M. and Al Zahrani, S.M. (2018) Effect of Date Palm Fiber Loadings on the Mechanical Properties of High Density Polyethylene/Date Palm Fiber Composites. *Key Engineering Materials*, **773**, 94-99. <https://doi.org/10.4028/www.scientific.net/KEM.773.94>
- [14] Ghazi, I.F. and Jaddan, R.I. (2021) Thermal Conductivity Characterization of Epoxy Based Composites Reinforced with Date Palm Waste Particles. *Journal of Physics: Conference Series*, **1973**, Article ID: 012144. <https://doi.org/10.1088/1742-6596/1973/1/012144>
- [15] Saad Azzem, L. and Bellel, N. (2022) Thermal and Physico-Chemical Characteristics of Plaster Reinforced with Wheat Straw for Use as Insulating Materials in Building. *Buildings*, **12**, Article No. 1119. <https://doi.org/10.3390/buildings12081119>
- [16] El-Sayed Ali, M. and Zeitoun, O.M. (2012) Discovering and Manufacturing a New Natural Insulating Material Extracted from a Plant Growing up in Saudi Arabia. *Journal of Engineered Fibers and Fabrics*, **7**, 88-94. <https://doi.org/10.1177/155892501200700405>
- [17] Ali, M.E. and Alabdulkarem, A. (2017) On Thermal Characteristics and Microstructure of a New Insulation Material Extracted from Date Palm Trees Surface Fibers. *Construction and Building Materials*, **138**, 276-284. <https://doi.org/10.1016/j.conbuildmat.2017.02.012>
- [18] Ali, M., Alabdulkarem, A., Nuhait, A., Al-Salem, K., Iannace, G., Almuzaiker, R., et al. (2020) Thermal and Acoustic Characteristics of Novel Thermal Insulating Materials Made of Eucalyptus Globulus Leaves and Wheat Straw Fibers. *Journal of Building Engineering*, **32**, Article ID: 101452. <https://doi.org/10.1016/j.jobbe.2020.101452>
- [19] Soviwadan, D., Kassegne, K.A. and Komla, S. (2015) Elaboration et caracterisation mecanique et physique des panneaux de particules de sciure de kapokier avec la poudre tanifere de la cosse deousse de nere. *European Scientific Journal*, **11**, 57-69.
- [20] Tido Tiwa, S. (2021) Earth-Based Construction Materials Reinforced with Tropical Plants and Recycled Waste Cellulose Pulp Fibre: Performance and Durability Assessment. Abuja, Nigeria.
- [21] Azzouz, F. (2015) Stabilisation des sols argileux de la region de tlemcen par les sels. *Revue Elwihat Pour Les Recherches et Les Etudes*, **8**, 108-117. <https://doi.org/10.54246/1548-008-001-060>
- [22] Abdelhalim, C., Melik, B. and Belgacem, B. (2022) Influence de l'ajoute de sable grossier sur la compressibilite du sol limoneux. *Le 1er Seminaire national de genie civil et des travaux publics*, Khenchela, Algérie, 15-16 Février 2022, 1-8.
- [23] Malbila, E., Djoko, B., Compaore, A., Toguyeni, D., Kam, S. and BathiÉBo, D.J. (2022) Experimental Study of Physical and Mechanical Properties of Concrete by Waste Glass Powder as Partial Replacement of Cement. *International Journal of Advanced Research (IJAR)*, **10**, 809-825. <https://doi.org/10.21474/IJAR01/15239>

- [24] Yoganandam, K., Ganeshan, P., NagarajaGanesh, B. and Raja, K. (2020) Characterization Studies on *Calotropis procera* Fibers and Their Performance as Reinforcements in Epoxy Matrix. *Journal of Natural Fibers*, **17**, 1706-1718. <https://doi.org/10.1080/15440478.2019.1588831>
- [25] Alabdulkarem, A., Ali, M., Iannace, G., Sadek, S. and Almuzaiqer, R. (2018) Thermal Analysis, Microstructure and Acoustic Characteristics of Some Hybrid Natural Insulating Materials. *Construction and Building Materials*, **187**, 185-196. <https://doi.org/10.1016/j.conbuildmat.2018.07.213>
- [26] Manuel Álvarez, D., Ferrández, P., Guijarro-Miragaya, C. and Morón (2023) Characterization and under Water Action Behaviour of a New Plaster-Based Lightened Composites for Precast. *Materials*, **16**, Article No. 872. <https://doi.org/10.3390/ma16020872>
- [27] Tagne, N.R.S., Mbou, T.E., Harzallah, O., Ndapeu, D., Huisken, W., Nkemaja, D., Njeugna, E., Fogue, M. and Drean, J.-Y. (2020) Physicochemical and Mechanical Characterization of *Raphia vinifera* Pith. *Advances in Materials Science and Engineering*, **2020**, Article ID: 8895913. <https://doi.org/10.1155/2020/8895913>
- [28] Daligand, D. (2002) Plâtre, technique de l'ingenieur traite construction. Vol. 3, 24. <https://doi.org/10.51257/a-v3-c910>
- [29] Meille, S. (2001) Etude du comportement mecanique du platre pris en relation avec sa microstructure. Lyon.
- [30] AFNOR (1993) Panneaux a base de bois—Determination de la masse volumique.
- [31] AFNOR (1993) EN 317, Particleboards and Fibreboards—Determination of Swelling in Thickness after Immersion in Water.
- [32] Toguyeni, D., Bathiebo, D. and Koulidiati, J. (2011) Etude experimentale, par la methode du plan chaud, des proprietes thermophysiques d'un bois tropical et d'un panneau isolant formule avec des intrants locaux. *Journal de la societe ouest-africaine de chimie*, No. 32, 18-26.
- [33] Ouédraogo, E., Coulibaly, O., Imbga, B.K., Kiéno, P.F. and Ouédraogo, A. (2018) Experimental Study of the Thermo-Physical Properties of Lateritic Blocks Used in the Habitat in Dry Tropical Climate. *Physical Science International Journal*, **19**, 1-10. <https://doi.org/10.9734/PSIJ/2018/43887>
- [34] Toussakoe, K., Ouedraogo, E., Imbga, K., Messan, A. and Kieno, F.P. (2021) Caracterisation mecanique et thermo-physique de l'adobe utilise dans la voute nubienne. *Afrique Science*, **19**, 186-199.
- [35] Malbila, E., Delvoie, S., Toguyeni, D., Attia, S. and Courard, L. (2020) An Experimental Study on the Use of Fonio Straw and Shea Butter Residue for Improving the Thermophysical and Mechanical Properties of Compressed Earth Blocks. *Journal of Minerals and Materials Characterization and Engineering*, **8**, 107-132. <https://doi.org/10.4236/jmmce.2020.83008>
- [36] Mohamed, L., Mohamed, K., Najma, L. and Abdelhamid, K. (2018) Thermal Characterization of a New Effective Building Material Based on Clay and Olive Waste. *MATEC Web of Conferences*, **149**, Article No. 02053. <https://doi.org/10.1051/mateconf/201814902053>
- [37] AFnor (1982) NF p18-411, betons—caracteristiques communes des machines hydrauliques pour essais de compression, flexion et traction des materiaux durs.
- [38] EN 12089 (2013) European Standard Test Method for Thermal Insulating Products for Building Applications—Determination of Bending Behaviour. European Committee for Standardization, Brussels.
- [39] RILEM-TC (1984) Test for the Determination of Modulus of Rupture and Limit of

- Proportionality of Thin Fibre Reinforced Cement Sections. In: *RILEM Recommendations for the Testing and Use of Construction Materials*, RILEM (Ed.) E & F SPON, London, 161-163.
- [40] Salas-Ruiz, A., Barbero-Barrera, M.M. and Ruiz-TÉLlez, T. (2019) Microstructural and Thermo-Physical Characterization of a Water Hyacinth Petiole for Thermal Insulation Particle Board Manufacture. *Materials*, **12**, Article No. 560. <https://doi.org/10.3390/ma12040560>
- [41] ANSI A 208 1 (1999) Medium Density Fibreboard. National Particleboard Association, Gaithersburg, 11 p.
- [42] Zaragoza-Benzal, A., Ferrandez, D., Diaz-Velilla, J.P. and ZÚNiga, J.A. (2023) Manufacture and Characterisation of a New Lightweight Plaster for Application in Wet Rooms under Circular Economy Criteria. *Case Studies in Construction Materials*, **19**, e02380. <https://doi.org/10.1016/j.cscm.2023.e02380>
- [43] Manjit, S. and Mridul, C. (1992) Glass Fibre-Reinforced Water-Resistant Gypsum-Based Composite. *Cement Composites*, **14**, 23-32. [https://doi.org/10.1016/0958-9465\(92\)90036-U](https://doi.org/10.1016/0958-9465(92)90036-U)
- [44] Al-Homoud Mohammad, S. (2005) Performance Characteristics and Practical Applications of Common Building Thermal Insulation Materials. *Building and Environment*, **40**, 353-366. <https://doi.org/10.1016/j.buildenv.2004.05.013>
- [45] Zaragoza-Benzal, A., Ferrández, D., Santos, P. and Morón, C. (2023) Recovery of End-of-Life Tyres and Mineral Wool Waste: A Case Study with Gypsum Composite Materials Applying Circular Economy Criteria. *Materials*, **16**, Article No. 243. <https://doi.org/10.3390/ma16010243>
- [46] EN 13279-2 (2014) Gypsum Binders and Gypsum Plasters—Part 2: Test Methods.
- [47] Vidil, L. (2019) Etude de materiaux naturels 2d-potentialites d'utilisation comme renfort de materiaux composites.
- [48] Pierre and Dalmay (2009) Etude physico-chimique et mecanique de composites a matrice platre contenant des fibres vegetales. Limoges (France).
- [49] Rao, D. and Kumar, S. (2017) Mechanical Behaviour of Hybrid Bio-Composite Reinforced with Walnut (*Juglans regia* L.) Shell Particle and Coconut Fibre. *International Journal on Emerging Technologies*, **8**, 604-608.
- [50] Yamossou, G.G. (2010) Mise au point d'un ecomateriau a vocation d'isolation thermique. Ouagadougou.
- [51] Ebanda, F.B. (2012) Etude des proprietes mecaniques et thermiques du platre renforce de fibres vegetales tropicales. Clermont-Ferrand.

Nomenclature

b	Width of the sample (mm);
L	Span (mm);
F	Load applied (N);
d	Thickness of the sample (mm).
σ_f	Flexure stress (MPa)
ρ_{real}	Real density (g/cm^3)
m_f	Final mass of the sample(g)
m_i	Initial mass of the sample (g)
ω_h	Moisture absorption rate (%)
V_f	Final volume (cm^3)
V_i	Initial volume (cm^3)
m_e	Specimen mass (g)
m_{e+p}	Mass of the waxed specimen (g)
ρ_p	Paraffin density(g/cm^3)
V_p	Paraffin volume (cm^3)
L	Length of the specimen (cm)
I	Width of the specimen, (cm);
e	Thickness of the specimen (cm).
ρ_{ap}	Bulk mass(g/cm^3)
m	Mass, (g)
V	volume (cm^3)
T	Particles size
θ_1	Laplace transform of the temperature $T_1(t)$
Φ_1	Laplace transform of the heat flux from the probe to the sample at the top
Φ_2	Laplace transform of the heat flow from the probe to the insulator (Polystyrene) downwards
Φ_0	Laplace transforms of the total fluxes emitted by the probe towards the sample (top) and towards the insulation (polystyrene) at the bottom
C_s	Surface heat capacity of the probe
R_c	Contact resistance between the sample and the probe
e_1	Thicknesses of the insulation
e	Thicknesses of the sample
a_i	Thermal diffusivity of polystyrene
$t_{i,Mn}$	Interior temperature of the model without insulation
$t_{i,Mi}$	Interior temperature of the model with insulation
t_2, t_3	Outside temperature of the models
RVP	Raffia Vinifera Particles